University of Texas at Arlington
MavMatrix

2022 Spring Honors Capstone Projects | Honors College

5-1-2022

Fabrication of a Microfluidic System to Generate Micro-carrier Beads for Cell Culture

Giles Fitzwilliams

Follow this and additional works at: https://mavmatrix.uta.edu/honors_spring2022

Recommended Citation

Fitzwilliams, Giles, "Fabrication of a Microfluidic System to Generate Micro-carrier Beads for Cell Culture" (2022). *2022 Spring Honors Capstone Projects*. 58.
https://mavmatrix.uta.edu/honors_spring2022/58

This Honors Thesis is brought to you for free and open access by the Honors College at MavMatrix. It has been accepted for inclusion in 2022 Spring Honors Capstone Projects by an authorized administrator of MavMatrix. For more information, please contact leah.mccurdy@uta.edu, erica.rousseau@uta.edu, vanessa.garrett@uta.edu.

Copyright © by Giles Fitzwilliams 2022

All Rights Reserved

FABRICATION OF A MICROFLUIDIC SYSTEM TO GENERATE MICRO-CARRIER BEADS FOR CELL CULTURE

by

GILES FITZWILLIAMS

Presented to the Faculty of the Honors College of

The University of Texas at Arlington in Partial Fulfillment

of the Requirements

for the Degree of

HONORS BACHELOR OF SCIENCE IN BIOMEDICAL ENGINEERING

THE UNIVERSITY OF TEXAS AT ARLINGTON

May 2022

ACKNOWLEDGMENTS

I would like to first thank my mentor, Dr. Hong, for his guidance throughout this whole project. His recommendations and encouragement to take initiative was greatly appreciated. I would also like to thank my group members, Mohammad Abu Khoder and Isabella Solorzano, for their dedication and contribution to this project. Lastly, I would like to thank the graduate students, Alan Taylor and Jiazhu Xu, for their availability to work with the project team and assist us with any materials we needed to run the experiment.

May 3, 2022

ABSTRACT

FABRICAITON OF A MICROFLUIDIC SYSTEM TO GENERATE MICRO-CARRIER BEADS FOR CELL CULTURE

Giles Fitzwilliams, B.S. Biomedical Engineering

The University of Texas at Arlington, 2022

Faculty Mentor: Yi Hong

Current procedures used to make microfluidic systems can range up to thousands of dollars. The objective of this project was to create a cost-effective four inlet microfluidic system that can produce uniform microcarrier beads ranging from 100 μm to 1000 μm in diameter. To create this device, research was done on sodium alginate and gelatin, bead components, properties, and their interactions with one another within a microfluidic system. The device was fabricated using a 3D printed acrylonitrile butadiene styrene (ABS) plastic design mold and encasing the mold in a polydimethylsiloxane (PDMS). After cleaning the device with acetone, Harvard syringe pumps were used to inject sodium alginate, gelatin, and oil and varying flow rates to produce microcarrier beads. It was found

that device was able to produce uniform beads that decreased in diameter as the oil flow rate increased.

TABLE OF CONTENTS

ACKNOWLEDGMENTS iii

ABSTRACT iv

LIST OF ILLUSTRATIONS viii

Chapter

1. INTRODUCTION 1

    1.1 Microfluidic Systems 1

    1.2 Microfluidic System Build and Principles 1

    1.3 Honors Contribution 2

2. LITERATURE REVIEW 3

    2.1 Microfluidic System Contributions 3

        2.1.1 Low Reagent Consumption 3

        2.1.2 High Surface Area Availability 3

        2.1.3 High-Throughput Production 4

    2.2 Microfluidic System Fabrication 4

    2.3 Microfluidic Principles 5

3. METHODOLOGY 7

    3.1 Fabrication 7

        3.1.1 Printing of the Channel Scaffold 7

        3.1.2 PDMS Preparation 8

3.1.3 Removal of 3D Printed Scaffold from PDMS Device 8
3.2 Experimental Set-Up & Testing 8
4. RESULTS 10
4.1 Microcarrier Bead Diameter Analysis 10
4.1.1 Microcarrier Bead Representative Bead Pictures 11
4.1.1.1 Flow Rate Ratio of 10,000µl/hr:1000µl/hr (10 to 1) 11
4.1.1.2 Flow Rate Ratio of 30,000µl/hr:1000µl/hr (30 to 1) 11
4.1.1.3 Flow Rate Ratio of 50,000µl/hr:1000µl/hr (50 to 1) 12
4.1.1.4 Flow Rate Ratio of 60,000µl/hr:1000µl/hr (60 to 1) 12
4.1.1.5 Flow Rate Ratio of 75,000µl/hr:1000µl/hr (75 to 1) 12
4.1.1.6 Flow Rate Ratio of 100,000µl/hr:1000µl/hr (100 to 1) 13
5. CONCLUSION & DISCUSSION 14
5.1 Results Analysis 14
5.2 Microfluidic Device Assessment 14
5.3 Environmental Impact of Project Device 15
Appendix
A. ADDITIONAL BEADS IMAGED FOR DATA ANALYSIS 16
REFERENCES 21
BIOGRAPHICAL INFORMATION 24

LIST OF ILLUSTRATIONS

Figure		Page
2.1	Depiction of Photolithography	5
2.2	Display of the Various Flow Regimes	6
3.1	Experimental Set-Up of the Project Microfluidic System	9
4.1	Experimental Results of Bead Size vs. Flow Rate Ratio	10
4.2	Microcarrier Beads Produced at a 10 to 1 Flow Rate Ratio	11
4.3	Microcarrier Beads Produced at a 30 to 1 Flow Rate Ratio	11
4.4	Microcarrier Beads Produced at a 50 to 1 Flow Rate Ratio	12
4.5	Microcarrier Beads Produced at a 60 to 1 Flow Rate Ratio	12
4.6	Microcarrier Beads Produced at a 75 to 1 Flow Rate Ratio	12
4.7	Microcarrier Beads Produced at a 100 to 1 Flow Rate Ratio	13

CHAPTER 1

INTRODUCTION

1.1 Microfluidic Systems

Microfluidic systems are best known as biological tools used in the fields of tissue engineering and drug delivery. These devices aid in the creation of microcarriers which are utilized in the proliferation and differentiation of cells. The microcarriers' high surface area is also a good environment for cell growth due to the exceptionally low toxicity. Microfluidic systems can also analyze DNA or detect the makeup of various fluids.

1.2 Microfluidic System Build and Principles

The overall system is a combination of channels in unique designs that are either fabricated using a mold or they are created on a chip. The channels converge and have inputs in which various fluids can amalgamate into a uniform product. The manipulation of the fluids within the system is the result of numerous parameters of the system. These parameters include a valve system within the system design, or the manipulation of a pressure controller put into the system.

The principle behind generating the microcarrier beads at varying lengths is based on jetting regimes. The jetting regime allows for the alteration of droplet formation sizes based on the speed of the fluids. There is a constant and disperse phase of fluids. The higher the speed of the constant phase fluid, the smaller the droplet sizes are from the system. In contrast, the slower the constant phase fluid, the bigger the droplet size. It is this principle that will be the foundation for the creation of different microcarrier bead diameters.

1.3 Honors Contribution

The required Honors contribution for this project was to do additional research on the fluid techniques and models the group could use to help aid the production of the microcarrier beads. The formation and shape of the microcarrier beads rely on an understanding of fluid dynamics that can occur within a microfluidic system. The research found was implemented and used to help create a proper experimental set-up with the device to create uniform-shaped beads that could be then used for future 3D cell culture models. 3D cell culture models can aid in the promotion of unique cell morphology and growth parallel to that of the human body. In vitro models that are like the human body can help researchers grasp a better understanding of the chemical and physical interactions that take place amongst cancer and or healthy cells.

CHAPTER 2

LITERATURE REVIEW

2.1 Microfluidic System Contributions

Microfluidics holds a potentially integral part in the evolution of biotechnology research. Microfluidic systems are looked upon as a "lab-on-a-chip," meaning that they have the potential to be used for high throughput testing in data analysis and quantitative measurements. Benefits from the use of microfluidic technology include cell morphology analysis, co-culture assays, and microbial population analysis (Ortseifen et al., 2020). The technology of microfluidic systems is still only a decade old and has yet to truly be embraced within most biological labs. However, microfluidic systems can provide a wide range of benefits. These benefits include low reagent consumption, high surface area availability, and high-throughput production.

2.1.1 Low Reagent Consumption

Microfluidic systems do not require a high volume of reagents for testing, because the system is usually made at a small scale (Krauss, 2019). This creates a decline in cost for performing certain experiments. The small scale also simplifies the analysis of components that are difficult to obtain through purification or use of hazardous reagents.

2.1.2 High Surface Area Availability

The channel fabrications of the microfluidic systems allow for fast transportation and interactions. This is applicable for surface interaction reactions such as component

mixture for microbead fabrication, immobilized enzyme applications, or sensing / detection applications (Gervais and Jensen, 2006).

2.1.3 High-Throughput Production

High-throughput experiments can be tested via droplet microfluidics. These microfluidic devices that execute creating small droplets that can be screened individually. The speed at which the droplets get produced can also easily be manipulated by system flow rate parameters. The droplet can encapsulate cells or enzymes and create an environment of high concentrations while remaining at a microscopic size (Colin et al., 2015).

2.2 Microfluidic System Fabrication

There are numerous ways in which a microfluidic device can be fabricated. These methods can include ultrasonic machining, laser ablation, focused ion beam machining, and photolithography (Scott and Ali, 2021). Photolithography is the method most similar to the project's method of fabrication in the sense of using a polymer for fabrication. The method of fabrication lithography stated in most literature follows coating a silicon wafer with a photoresist material. A photomask is then used to create a shape as UV light is exposed to the wafer. The wafer is then baked and rinsed. A polymer known as polydimethylsiloxane (PDMS) is then casted over the silicon wafer at a certain temperature. Once the PDMS has cured, it is removed from the wafer. The device can then be observed with its impression of the silicon pattern.

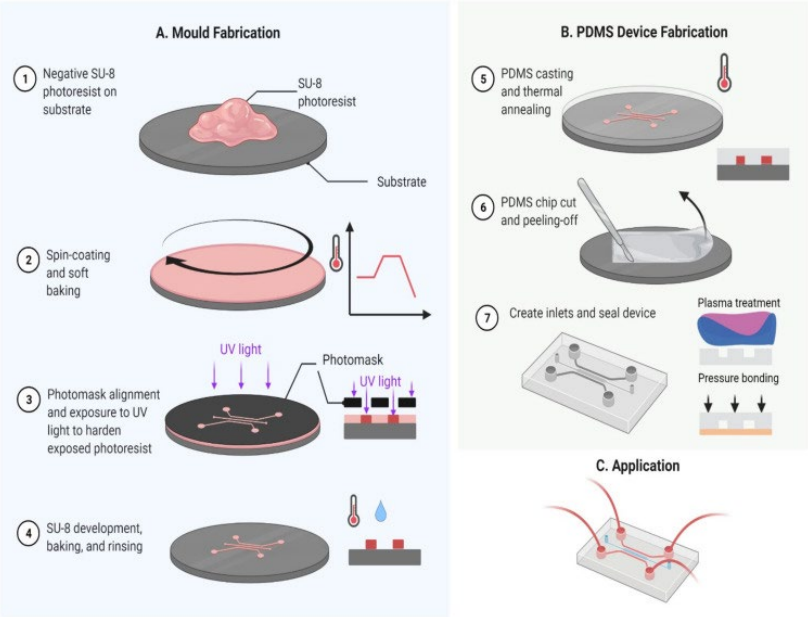

Figure 2.1: Depiction of Photolithography

2.3 Microfluidic Principles

Microfluidic systems follow different flow regime models. All these models manipulate the interface between what is known as a continuous phase and dispersed phase. The dispersed phase is the particle or droplet that is formed within the microfluidic system. The continuous phase surrounds the dispersed phase to encapsulate the droplets as they exit the microfluidic system. Most of the notable regimes include dripping, jetting, and flow focused. Dripping regimes follow an accumulation of the solution at the end of the tube and then eventual detachment of the droplets (Shen et al., 2020). The principle of the droplet size via the droplet regime is based upon the radius of the tubing of the device and the droplet length. The jetting regime follows a method of the droplet being formed after a far extension from the end of the tube due to a high velocity of the dispersed phase. Inertial force from such a high velocity creates detachment and formation of droplet (Shen et al., 2020). Lastly, a flow focused regime focusing on manipulating the flow rates of the constant phase and dispersed phase to create highly monodisperse droplets (Shih et al.,

2013). In the flow focused regime, the constant phase can be manipulated at faster or slower flow rates while the dispersed phase is kept at a constant flow rate. The faster the continuous phase the smaller the particles formed.

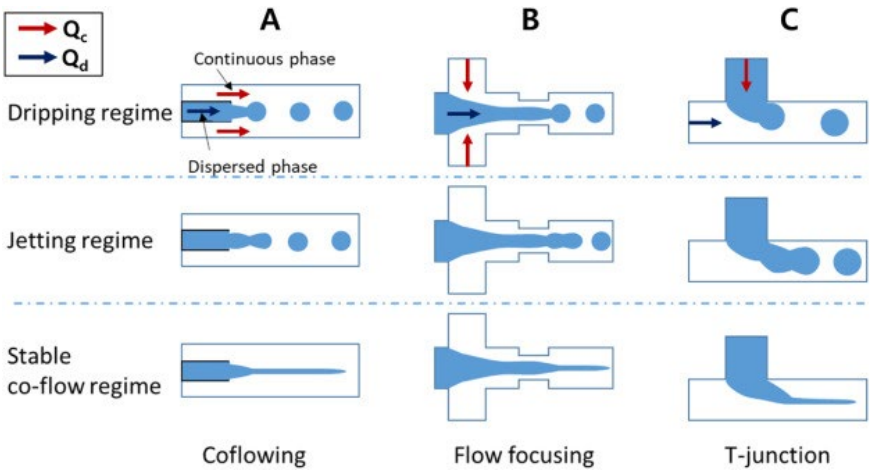

Figure 2.2: Display of the Various Flow Regimes

CHAPTER 3

METHODOLOGY

3.1 Fabrication

To fabricate the microfluidic system, a Sylgard 184 PDMS solution kit was used. PDMS was used due to its good elasticity, inertness to various chemicals, and accessibility. The Sylgard Kit is composed of two parts: the pre-polymer base and the cross-linking agent. The ratio between the pre-polymer base and cross-linking agent is ten to one.

There are several techniques for fabricating microfluidic systems using PDMS, such as mold injection, which reduces the fabrication process, but this method needs a fabricated mold that will withstand a curing temperature of 80 ºC. Another technique is the soft-lithography method, which was used as the fabrication technique in the project after discussing both techniques with the project mentor, Dr. Hong.

The soft-lithography technique is a simple and straightforward method for fabrication of microfluidic systems and is commonly used and inexpensive; however, it requires more processing time. The fabrication process will be divided into four steps: 1) 3D printing the channel scaffold, 2) preparing the first layer of PDMS (bottom layer), 3) preparing the second layer of PDMS (top layer), and 4) Removing the 3D printed scaffold from the PDMS device.

3.1.1 3D Printing of the Channel Scaffold

SolidWorks was used to design the channels of the device with geometric characteristics. The channel molds and beds were 3D printed at UTA FabLab using ABS

plastic. The reason for choosing ABS plastic is because it is inexpensive ($0.05/g), easy to fabricate, and has good thermal properties compared to other materials like Polypropylene. ABS has a glass transition temperature of 105 °C and melting temperature of 230 °C, which is good since the PDMS system was incubated for two hours at 80 °C, which will not affect the ABS.

3.1.2 PDMS Preparation

After the ABS channel scaffold was fabricated, the first layer of PDMS was prepared by mixing 30ml of the pre-polymer with 3ml of the cross-linking agent from the PDMS kit. The first layer was then incubated for 20 minutes at 80 °C. This layer served as a foundation in which the ABS scaffold was placed on after it was cured. The channel ABS mold was placed on the first layer and then another 30ml of PDMS mixed solution was poured on top and cured for one hour at 80 °C.

3.1.3 Removal of 3D Printed Scaffold from PDMS Device

Removal of the ABS plastic took place by soaking the device in acetone solution overnight to create the hollow channels within the device. The acetone was utilized to soften and breakdown the ABS particles, which were then easily flushed by pumping more acetone in the channels using a syringe. There was no swelling or damage to the device.

3.2 Experiment Set-Up & Testing

The microfluidic device was composed of only one piece that contained four inlets and one outlet. The device was then connected to two Harvard PHD 2000 Syringe Pumps. Each pump has two outlet syringes. Each syringe outlet of pump one contained the prepared water-based solutions, 2% alginate and 1.5% gelatin, while the other pump contained vegetable oil.

Two 10ml syringes were filled, one with alginate and the second with gelatin were inserted into specific inlets. Two 20 ml syringes were filled with vegetable oil to function as the continuous phase and were inserted to their designated inlets. A prepared 5% calcium chloride solution was placed in a beaker on the stirring plate with a stirring magnet, a 1.5% glutaraldehyde solution was placed into another beaker and put aside until beads were ready to be placed in it. Food coloring was used to observe the mixing of the polymers. Gelatin was mixed with orange color, and alginate with blue coloring. The respective pumps for the alginate and gelatin and oil had flow rates entered to manipulate the produced microcarrier bead diameter sizes.

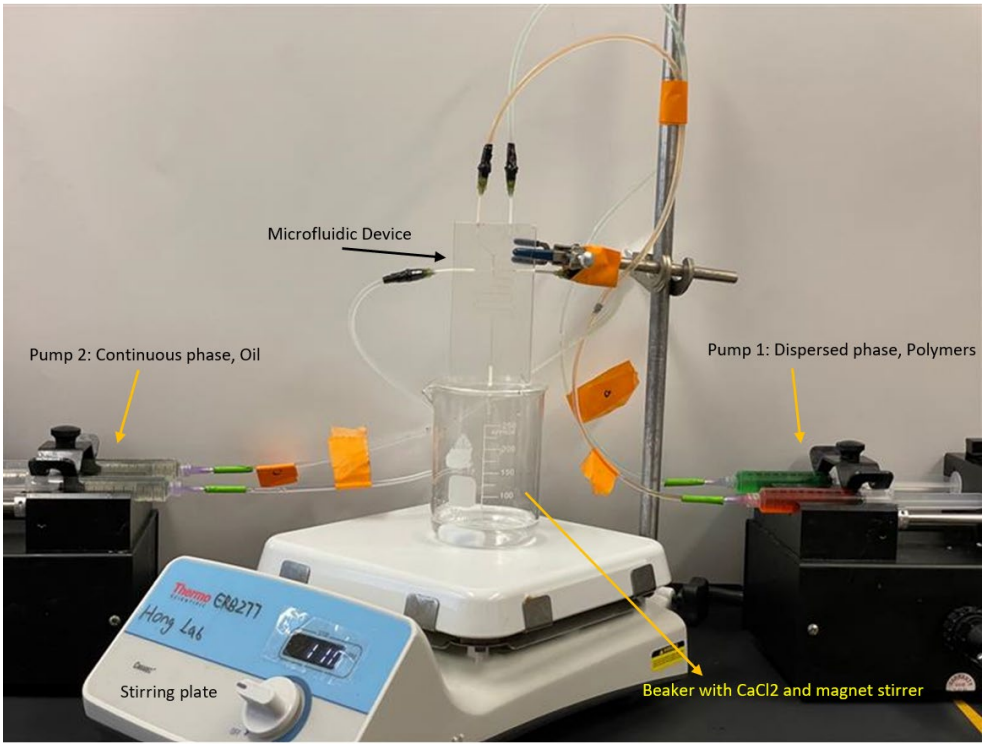

Figure 3.1: Experimental Set-Up of the Project Microfluidic System

CHAPTER 4

RESULTS

The results for this project were obtained using the software ImageJ to measure the diameters of the beads produced at various flow rates. The result that will be shown in this report are from the last experimental trial ran for this project. Six flow rate ratios were tested to fabricate microcarrier beads in the requested range of 100 µm to 1000 µm.

4.1 Microcarrier Bead Diameter Analysis

The collected microcarrier beads were imaged using a light microscope with a 4X objective lens. The images were saved and further analyzed and measured on the software ImageJ to obtain the bead diameters at each of the flow rate ratios.

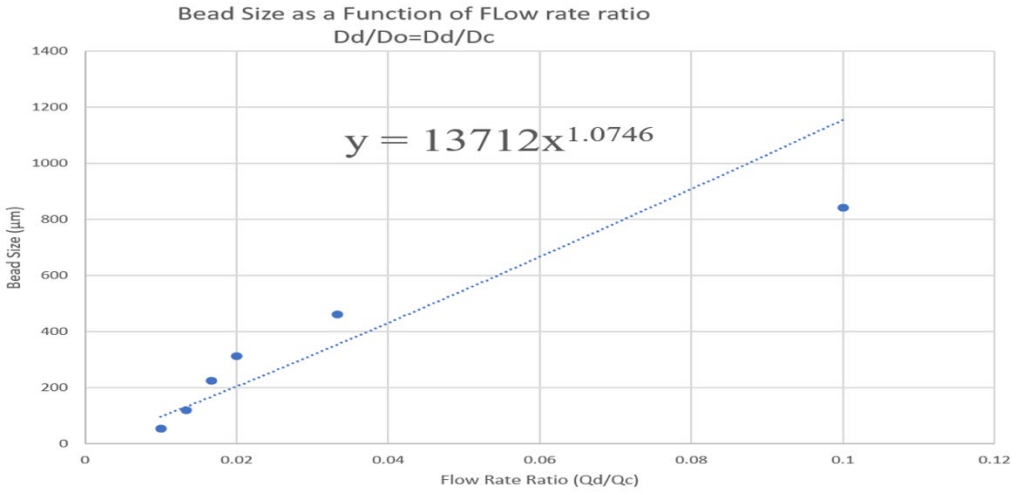

Figure 4.1: Experimental Results of Bead Size vs. Flow Rate Ratio

4.1.1 Microcarrier Bead Representative Bead Pictures

The following Images show the microcarrier beads produced at the six tested flow rate ratios. The flow rate ratio is in the format of the constant phase to dispersed phase.

4.1.1.1 Flow Rate Ratio of 10,000µl/hr:1000µl/hr (10 to 1)

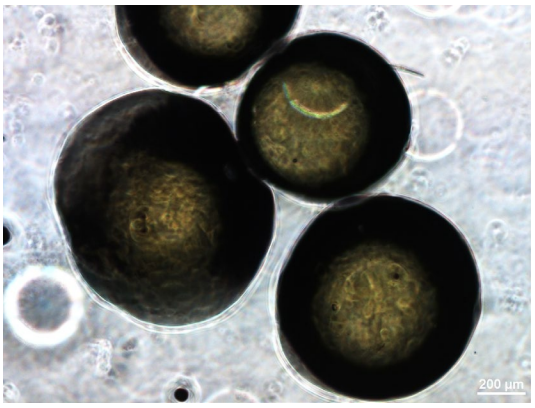

Figure 4.2: Microcarrier Beads Produced at a 10 to 1 Flow Rate Ratio

4.1.1.2 Flow Rate Ratio of 30,000µl/hr:1000µl/hr (30 to 1)

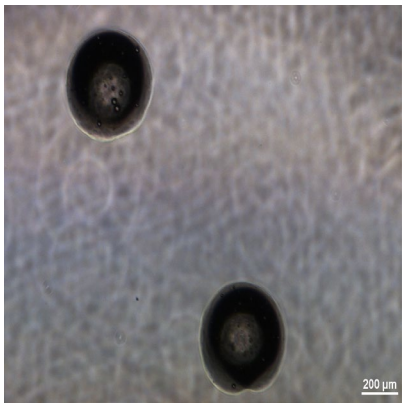

Figure 4.3: Microcarrier Beads Produced at a 30 to 1 Flow Rate Ratio

4.1.1.3 Flow Rate Ratio of 50,000µl/hr:1000µl/hr (50 to 1)

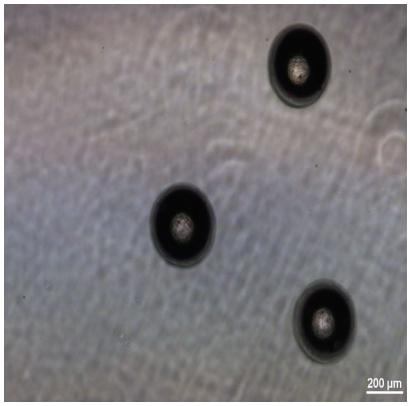

Figure 4.4: Microcarrier Beads Produced at a 50 to 1 Flow Fate Ratio

4.1.1.4 Flow Rate Ratio of 60,000µl/hr:1000µl/hr (60 to 1)

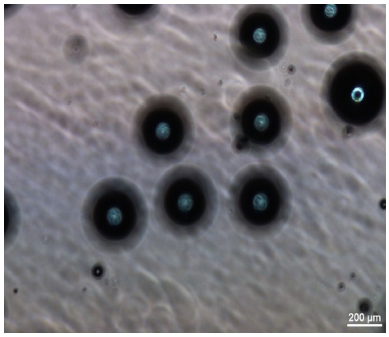

Figure 4.5: Microcarrier Beads Produced at a 60 to 1 Flow Rate Ratio

4.1.1.5 Flow Rate Ratio of 75,000µl/hr:1000µl/hr (75 to 1)

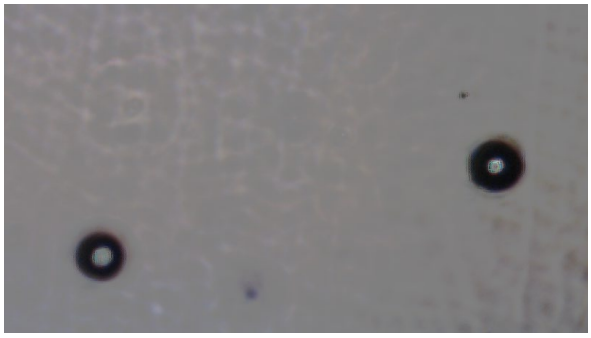

Figure 4.6: Microcarrier Beads Produced at a 75 to 1 Flow Rate Ratio

4.1.1.6 Flow Rate Ratio of 100,000µl/hr:1000µl/hr (100 to 1)

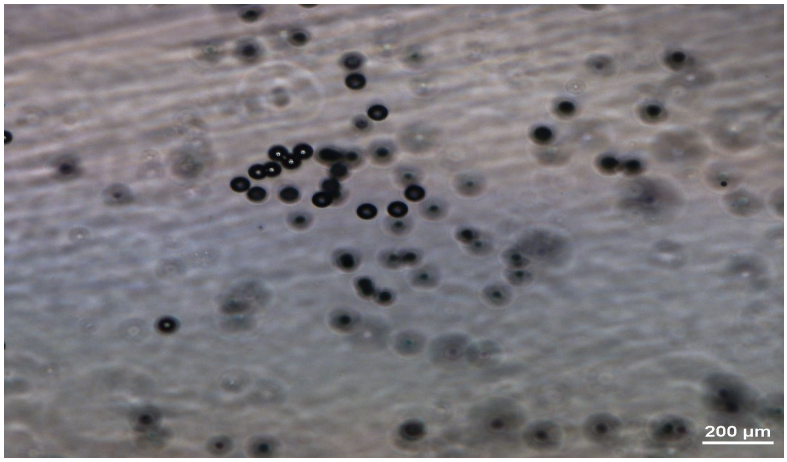

Figure 4.7: Microcarrier Beads Produced at a 100 to 1 Flow Rate Ratio

CHAPTER 5

CONCLUSION & DISCUSSION

Based on the results obtained from the performance evaluation, the device has successfully met both physical and functional requirements of the project. The size of the beads was controlled by manipulating the flowrate, all had uniform spherical shape, and they were a mixture of Alginate and Gelatin. The device itself is easy to use, made of a non-toxic clear plastic material PDMS and is reusable.

5.1 Results Analysis

Bead sizes at a flow rate ratio of 10:1 ranged from 741 μm to 920 μm and the average size was 840 μm ± 92 μm. At flow rate ratio of 30:1 the bead sizes ranged from 417 μm – 495 μm and the average was 461 μm ± 29 μm. The size of the beads at flow rate ratio of 50:1 ranged between 229 μm to 379 μm with an average of 312 μm ± 58μm. At the flow rate ratio of 60:1 the bead sizes ranged from 190 μm to 264 μm with an average of 224 μm ± 24 μm. Bead size decreased to almost half of the previous sizes at flow rate ratio of 75:1, ranging between 114 μm to 128 μm with average of 121 μm ± 9.8 μm. Finally, at flow rate ratio of 100:1 the beads size ranged between 47 μm to 61 μm with an average of 55 μm.

5.2 Microfluidic Device Assessment

The new results from the recent prototype showed successful fabrication of the beads. The device was able to produce microcarrier beads that ranged from 47 μm to approximately 920 μm in diameter. The beads were also uniform in shape and size within

each respective flow rate ratios of the constant and dispersed phase tested. This factor was especially important for this prototype, due to previous issues in maintaining a constant bead diameter on a certain flow rate ratio of the constant and dispersed phase. Another success of the device was seen in the proper mixing of sodium alginate and gelatin. The alteration of the gelatin concentration to match the density of sodium alginate, aided in proper mixing of the two components. Overall, it was concluded that the final iteration of the fabricated microfluidic device performs to the required functional specification.

5.3 Environmental Impact of Project Device

The device was fabricated out of PDMS, which is a durable and reusable material. However, the ability to make the channels within the PDMS system was made possible by utilizing ABS plastic, which is slightly toxic and releases chemical irritants when heated. There are several other plastic options available on the market that are not toxic, and more durable, such as PLA (polylactic acid). To add to this, the project also utilized several solutions to clear the system of obstructions and to crosslink the microcarrier beads. These solutions include calcium chloride, glutaraldehyde, and acetone. Calcium chloride is safe for environmental control, and glutaraldehyde is a biodegradable substance. Acetone, created industrially, is also listed as relatively environment friendly; however, high exposures of acetone can be harmful to aquatic life.

APPENDIX A

ADDITIONAL BEADS IMAGED FOR DATA ANALYSIS

Beads fabricated from a continuous phase to dispersed phase flow rate ratio of 30 to 1.

Bead Diameter Range: 437 µm – 482 µm

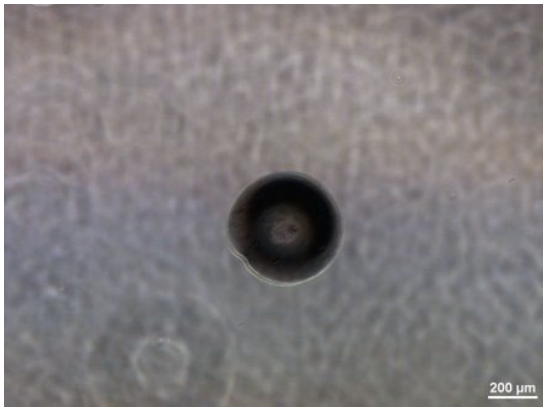

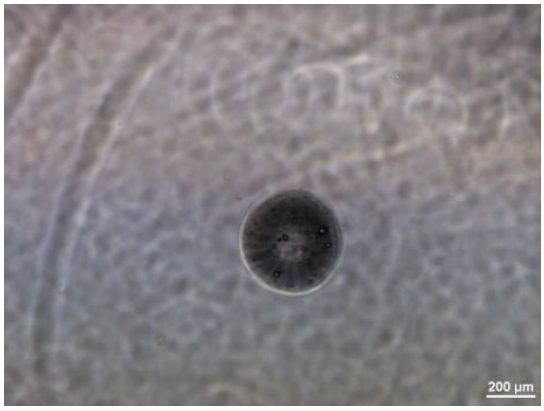

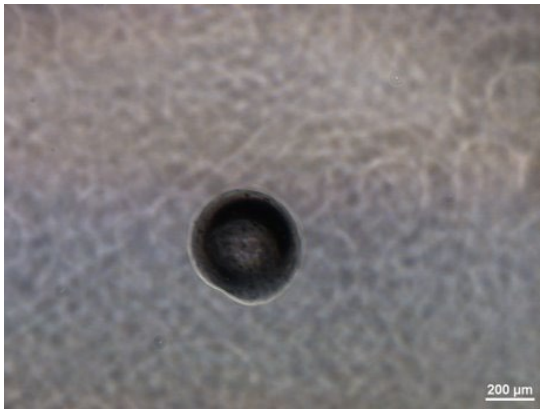

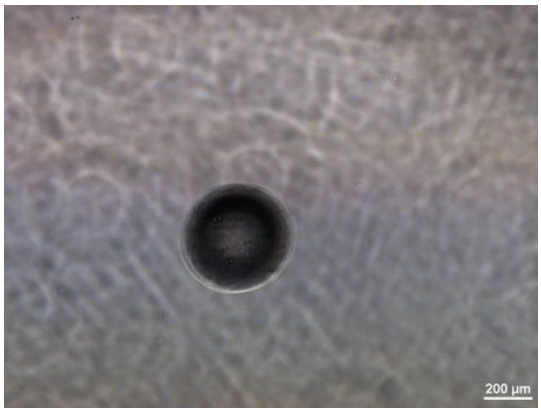

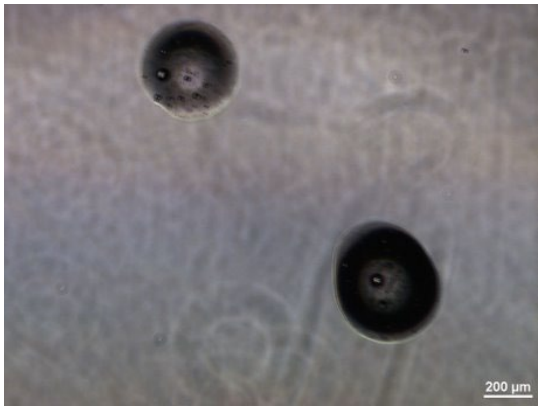

Beads fabricated from a continuous phase to dispersed phase flow rate ratio of 50 to 1.

Bead Diameter Range: 336 µm – 381 µm

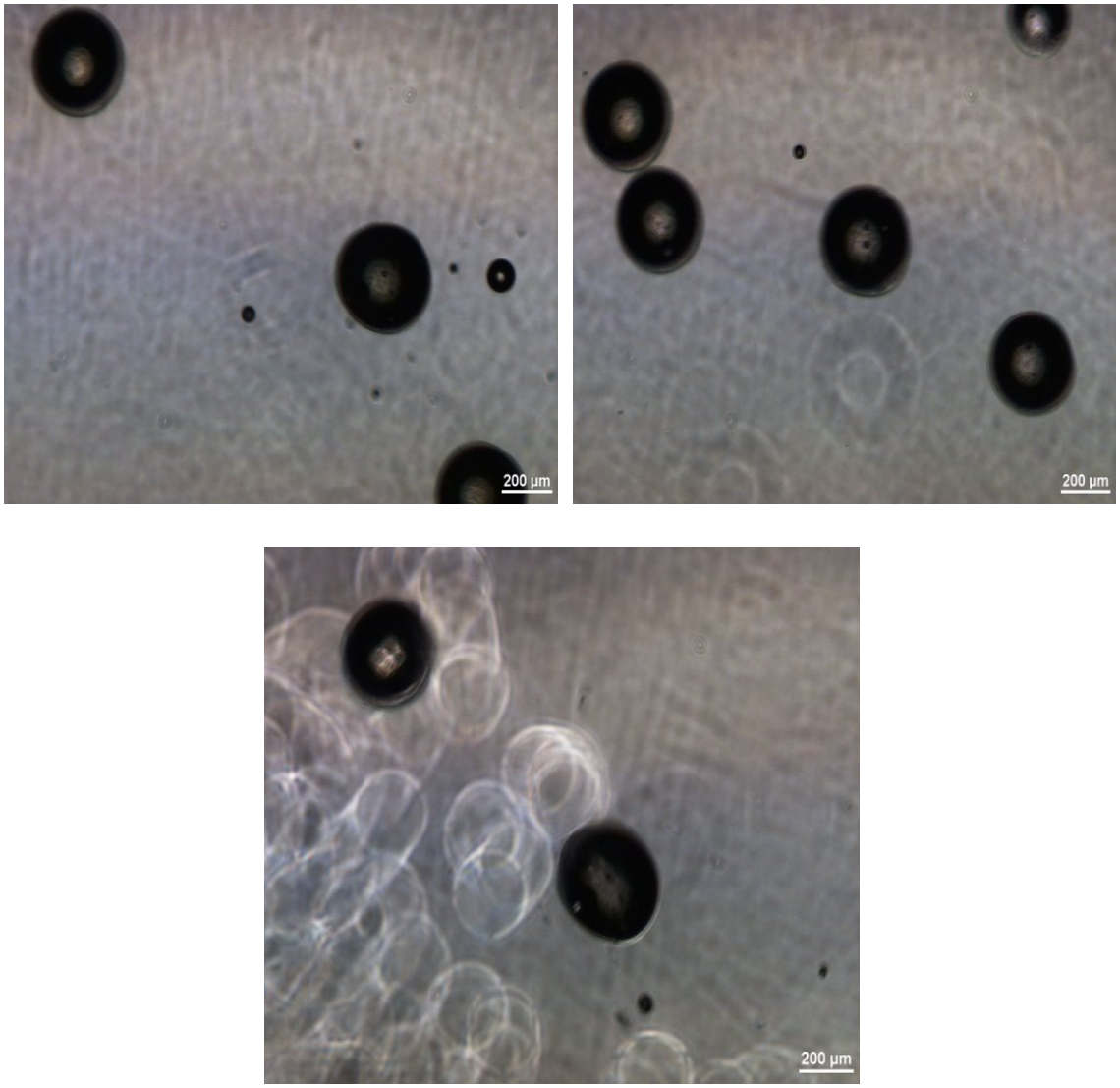

Beads fabricated from a continuous phase to dispersed phase flow rate ratio of 60 to 1.

Bead Diameter Range: 189 µm – 316 µm

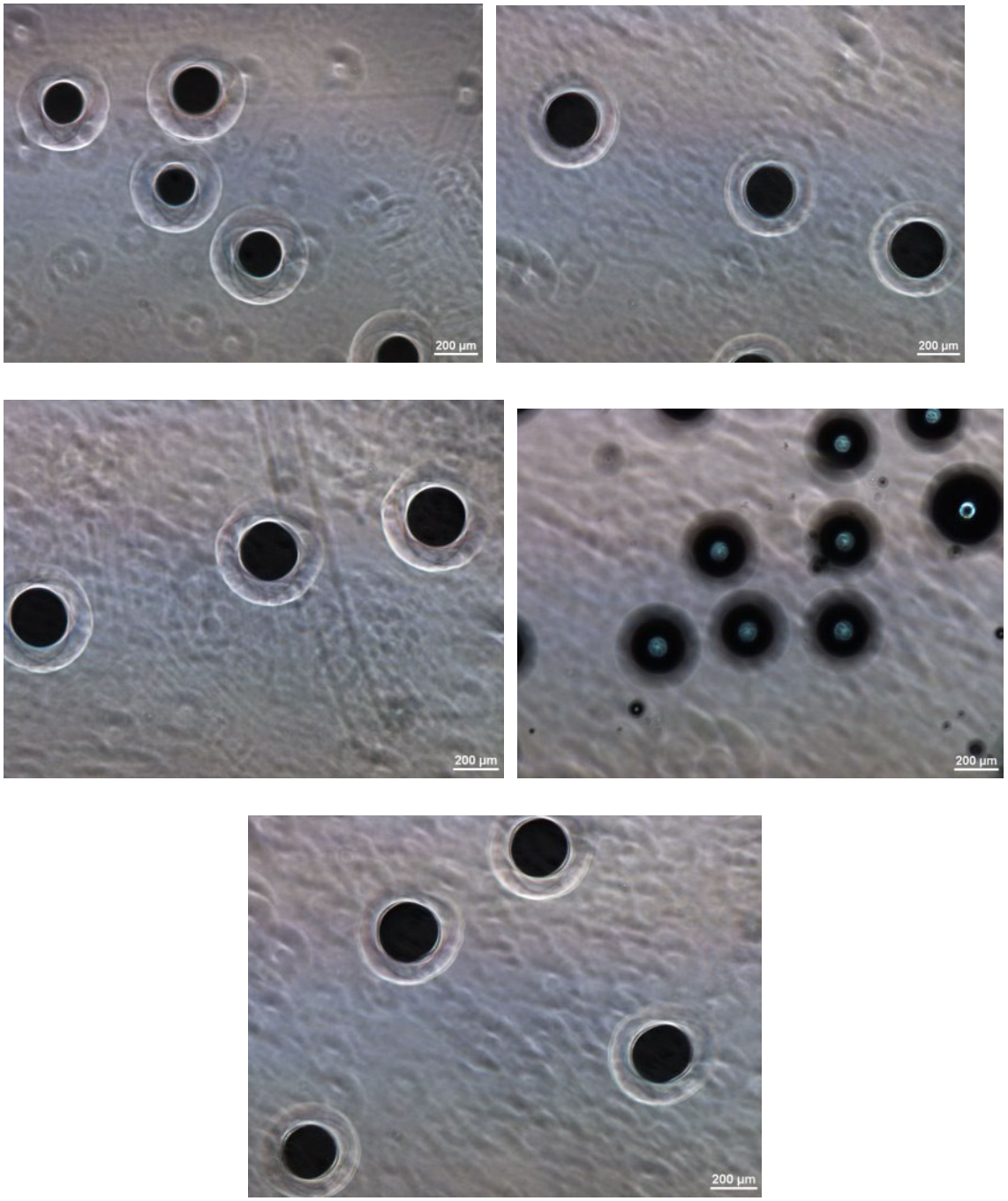

Beads fabricated from a continuous phase to dispersed phase flow rate ratio of 60 to 1.

Bead Diameter Range: 47 µm – 61 µm

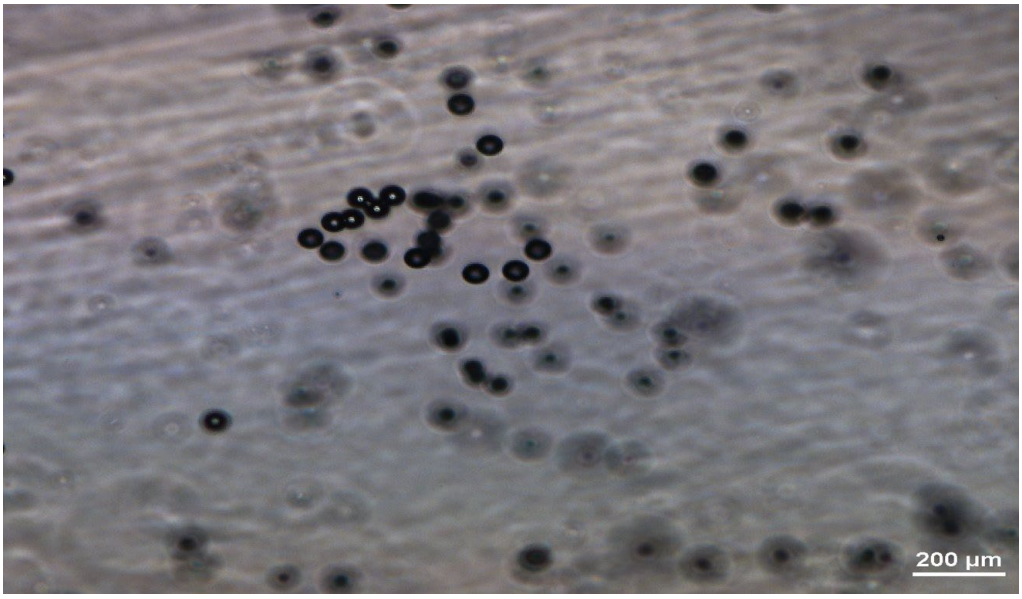

REFERENCES

Colin, P. Y., Kintses, B., Gielen, F., Miton, C. M., Fischer, G., Mohamed, M. F., Hyvönen, M., Morgavi, D. P., Janssen, D. B., & Hollfelder, F. (2015). Ultrahigh-throughput discovery of promiscuous enzymes by picodroplet functional metagenomics. *Nature Communications*, *6*(1). https://doi.org/10.1038/ncomms10008

Friend, J., & Yeo, L. (2010). Fabrication of microfluidic devices using polydimethylsiloxane. *Biomicrofluidics*, *4*(2), 026502. https://doi.org/10.1063/1.3259624

Fujii, T. (2002). PDMS-based microfluidic devices for biomedical applications. *Microelectronic Engineering*, *61–62*, 907–914. https://doi.org/10.1016/s0167-9317(02)00494-x

Gervais, T., & Jensen, K. F. (2006). Mass transport and surface reactions in microfluidic systems. *Chemical Engineering Science*, *61*(4), 1102–1121. https://doi.org/10.1016/j.ces.2005.06.024

Kang, K. K., Lee, B., & Lee, C. S. (2018). Microfluidic approaches for the design of functional materials. *Microelectronic Engineering*, *199*, 1–15. https://doi.org/10.1016/j.mee.2018.07.007

Ke, C. J., Chiu, K. H., Chen, C. Y., Huang, C. H., & Yao, C. H. (2021). Alginate-gelatin based core-shell capsule enhances the osteogenic potential of human osteoblast-like MG-63 cells. *Materials & Design*, *210*, 110109. https://doi.org/10.1016/j.matdes.2021.110109

Krauss, S. T., Woolf, M. S., Hadley, K. C., Collins, N. M., Nauman, A. Q., & Landers, J. P. (2019). Centrifugal microfluidic devices using low-volume reagent storage and inward fluid displacement for presumptive drug detection. *Sensors and Actuators B: Chemical*, *284*, 704–710. https://doi.org/10.1016/j.snb.2018.12.113

ŁAbowska, M. B., Cierluk, K., Jankowska, A. M., Kulbacka, J., Detyna, J., & Michalak, I. (2021). A Review on the Adaption of Alginate-Gelatin Hydrogels for 3D Cultures and Bioprinting. *Materials*, *14*(4), 858. https://doi.org/10.3390/ma14040858

Ortseifen, V., Viefhues, M., Wobbe, L., & Grünberger, A. (2020). Microfluidics for Biotechnology: Bridging Gaps to Foster Microfluidic Applications. *Frontiers in Bioengineering and Biotechnology*, *8*. https://doi.org/10.3389/fbioe.2020.589074

Scott, S., & Ali, Z. (2021). Fabrication Methods for Microfluidic Devices: An Overview. *Micromachines*, *12*(3), 319. https://doi.org/10.3390/mi12030319

Shen, C., Liu, F., Wu, L., Yu, C., & Yu, W. (2020a). Dripping, Jetting and Regime Transition of Droplet Formation in a Buoyancy-Assisted Microfluidic Device. *Micromachines*, *11*(11), 962. https://doi.org/10.3390/mi11110962

Shen, C., Liu, F., Wu, L., Yu, C., & Yu, W. (2020b). Dripping, Jetting and Regime Transition of Droplet Formation in a Buoyancy-Assisted Microfluidic Device. *Micromachines*, *11*(11), 962. https://doi.org/10.3390/mi11110962

Shih, R., Bardin, D., Martz, T. D., Sheeran, P. S., Dayton, P. A., & Lee, A. P. (2013). Flow-focusing regimes for accelerated production of monodisperse drug-loadable microbubbles toward clinical-scale applications. *Lab on a Chip*, *13*(24), 4816. https://doi.org/10.1039/c3lc51016f

Wang, J., Cheng, Y., Yu, Y., Fu, F., Chen, Z., Zhao, Y., & Gu, Z. (2015). Microfluidic Generation of Porous Microcarriers for Three-Dimensional Cell Culture. *ACS Applied Materials & Interfaces*, *7*(49), 27035–27039. https://doi.org/10.1021/acsami.5b10442

BIOGRAPHICAL INFORMATION

Giles Fitzwilliams is pursuing an Honors Bachelor of Science in Biomedical Engineering at the University of Texas at Arlington. He will be graduating in May 2022. During his academic career he had the pleasure of working with Dr. Young-Tae Kim in the biomedical engineering department. In Dr. Kim's lab Giles had the chance to do research as a McNair School and sponsored College of Engineering Undergraduate Researcher. Most of Giles research interest was centered around working with high-throughput cancer cell models. More specifically, he worked with MDA-MB-231 (Breast cancer) cells, PC3 (Prostate cancer) cells, and human dermal fibroblasts (HDF) to study their interface interactions in a unique method of cell seeding. Giles is currently on the path of perusing medical school and is aiming to apply either this upcoming application cycle or the next cycle.